

## An Integrated Bioinformatics Analysis of the Potential Regulatory Effects of miR-21 on T-cell Related Target Genes in Multiple Sclerosis

Mostafa Manian<sup>1</sup>, Ehsan Sohrabi<sup>2</sup>, Nahid Eskandari<sup>3</sup>, Mohammad-Ali Assarehzadegan<sup>1,4</sup>,  
Gordon A. Ferns<sup>5</sup>, Mitra Nourbakhsh<sup>6</sup>, Mir Hadi Jazayeri<sup>1,4\*</sup>, and Reza Nedaeinia<sup>7\*</sup>

1. Department of Immunology, Faculty of Medicine, Iran University of Medical Sciences, Tehran, Iran

2. Department of Medical Genetics and Molecular Biology, Faculty of Medicine, Iran University of Medical Sciences, Tehran, Iran

3. Department of Immunology, Faculty of Medicine, Isfahan University of Medical Sciences, Isfahan, Iran

4. Immunology Research Center, Institute of Immunology and Infectious Diseases, Iran University of Medical Sciences, Tehran, Iran

5. Brighton and Sussex Medical School, Division of Medical Education, Falmer, Brighton BN1 9PH, Sussex, UK

6. Department of Biochemistry and Nutrition, Faculty of Medicine, Iran University of Medical Sciences, Tehran, Iran

7. Pediatric Inherited Diseases Research Center, Research Institute for Primordial Prevention of Non-Communicable Disease, Isfahan University of Medical Sciences, Isfahan, Iran

### Abstract

**Background:** Overexpression of miR-21 is a characteristic feature of patients with Multiple Sclerosis (MS) and is involved in gene regulation and the expression enhancement of pro-inflammatory factors including IFN $\gamma$  and TNF- $\alpha$  following stimulation of T-cells *via* the T Cell Receptor (TCR). In this study, a novel integrated bioinformatics analysis was used to obtain a better understanding of the involvement of miR-21 in the development of MS, its protein biomarker signatures, RNA levels, and drug interactions through existing microarray and RNA-seq datasets of MS.

**Methods:** In order to obtain data on the Differentially Expressed Genes (DEGs) in patients with MS and normal controls, the GEO2R web tool was used to analyze the Gene Expression Omnibus (GEO) datasets, and then Protein-Protein Interaction (PPI) networks of co-expressed DEGs were designed using STRING. A molecular network of miRNA-genes and drugs based on differentially expressed genes was created for T-cells of MS patients to identify the targets of miR-21, that may act as important regulators and potential biomarkers for early diagnosis, prognosis and, potential therapeutic targets for MS.

**Results:** It found that seven genes (NR1P1, ARNT, KDM7A, S100A10, AK2, TGF $\beta$ R2, and IL-6R) are regulated by drugs used in MS and miR-21. Finally, three overlapping genes (S100A10, NR1P1, KDM7A) were identified between miRNA-gene-drug network and nineteen genes as hub genes which can reflect the pathophysiology of MS.

**Conclusion:** Our findings suggest that miR-21 and MS-related drugs can act synergistically to regulate several genes in the existing datasets, and miR-21 inhibitors have the potential to be used in MS treatment.

*Avicenna J Med Biotech 2021; 13(3): 149-165*

**Keywords:** Bioinformatics, MicroRNAs, Multiple sclerosis, T-cell

### Introduction

Multiple Sclerosis (MS) is a common neurological disorder, which is more prevalent in women than men, and is identified by demyelination, chronic inflammation, and progressive neurological dysfunction<sup>1,2</sup>. The etiology of this chronic inflammatory disorder is unclear; however, acute interstitial inflammation of nerves and the presence of multifocal sclerotic plaques in different parts of the peripheral and central nervous

system are common manifestations<sup>3</sup>. A fundamental characteristic of MS is an antigen-specific autoimmune response<sup>4</sup>. MS is a polygenic disease in which each gene has a small effect on the overall risk<sup>5</sup>. Recent genome-wide association studies have identified about 100 gene variants that are associated with a predisposition to MS. Most of these genes are considered to play a role in immunity<sup>6</sup>. MicroRNAs have been proposed

#### \* Corresponding authors:

Mir Hadi Jazayeri, Ph.D., Iran University of Medical Sciences, Tehran, Iran

Reza Nedaeinia, Ph.D., Hezar Jerib street, Pediatric Inherited Diseases Research Center, Research Institute for Primordial Prevention of Non-Communicable Disease, Isfahan University of Medical Sciences, Isfahan, Iran

Tel: +98 21 88622652

#### E-mail:

Jazayeri.mh@iums.ac.ir,  
molecular\_biology@mail.mui.ac.ir,

Reza.nedaie@gmail.com

Received: 3 Oct 2020

Accepted: 16 Jan 2021

as biomarkers for the early detection of MS <sup>7,8</sup>. Mature miRNAs are ~18–22 nucleotide single-stranded endogenous RNAs that bind to their target sequence on mRNA and regulate gene expression <sup>9</sup>. miRNAs are responsible for regulating the expression of more than 60% of mammalian protein-coding genes <sup>10</sup>. The expression profile of miRNA in MS patients has been studied and a large number of DEGs have been identified <sup>11</sup>. For example, there is strong evidence that miR-21 expression is up-regulated in MS patients compared with healthy controls <sup>12</sup>. These miRNAs are highly conserved non-coding RNAs involved in post-transcriptional regulation <sup>13</sup>. miRNAs appear to be potentially useful as diagnostic biomarkers for MS, and it has been shown that the differential expression of these miRNAs is dependent on the time of onset and therapeutic stage. Recent studies have demonstrated that miRNAs may also have essential roles in MS pathogenesis <sup>14</sup>. It is, therefore, possible that they could be used as both diagnostic markers and therapeutic targets in MS (Table 1) <sup>15,16</sup>. Although the function of miR-21 has been relatively well studied, its role in the development and progression of MS disease remains unclear. Satoh *et al* used proteomic profiling of MS brain lesions and analyzed the extracellular pathway to reveal the association between adhesion and integrin signaling in the progression of chronic MS lesions <sup>17</sup>. Freiesleben *et al* assessed microarray data of peripheral blood and integrated genes of MS patients using a consensus method that determines the degree of agreement of inconsistent data <sup>18</sup>. Studies performed using a variety of tissues such as brain lesions, and peripheral blood have been of relatively small cohort size and have not been replicated <sup>18</sup>. It is worth pointing out that this study investigated microarray profiling of miRNA of appropriate size patient cohort, introduced the approach of the molecular network, and generated consensus interaction network between differentially expressed miRNAs and genes in T-cells of untreated MS patients to identify dysregulated miRNAs and their

target genes. To study the complex heterogeneity of multiple sclerosis for identifying MS-associated molecular functional networks in cells and dysregulated molecular mechanisms and pathways, integrative analyses seem to be more efficient in identifying a potential therapeutic target than the assessment of individual genes <sup>6,19,20</sup>. Bioinformatics analysis of gene expression profiling has recently been used to identify genetic alterations at RNA level, and transcription factors can be applied as biomarkers for human diseases such as MS <sup>21</sup>. Bioinformatics analysis and systems biology can reveal molecular signatures comprising biomolecules at the protein level, drug, and RNA levels (miRNAs), and pathways have been used to obtain a more detailed understanding of the mechanisms involved in the pathogenesis of MS <sup>22,23</sup>. In the current study, a new integrated bioinformatics analysis was used to obtain a more detailed understanding of the mechanistic impact of miR-21 in MS, its protein biomarker signatures, RNA levels (mRNAs, miRNAs), and drug interactions by using the existing microarray databases of MS. MiR-21 was selected based on the reported dysregulation of this microRNA in MS <sup>24</sup>. Online databases such as HMDD v3.2, miR2Disease, and PhenomiR were used to determine the importance of miR-21 in gene regulation in MS. This study aimed to create a molecular network of miRNA genes and drugs, based on differentially expressed genes in T-cells of patients with MS, to identify the targets of miR-21, which act as important regulators and potential biomarkers in the early diagnosis, prognosis, and potential therapeutic targets for MS.

**Materials and Methods**

*Data collection for gene expression analysis*

Using a consistent specific platform, microarray datasets containing raw or normalized data were collected from the Gene Expression Omnibus (GEO) database. In order to collect comprehensive information, "multiple sclerosis", "Homo sapiens", and study type (Ex-

Table 1. An overview of the role of miR-21 in multiple sclerosis

| Authors                            | Year | miR-21 function   |
|------------------------------------|------|---|
| Ma <i>et al</i> (25)               | 2014 | - Up-regulated in peripheral blood mononuclear cells of relapsing-remitting MS patients<br>- Expansion of Th1 and Th17 cells<br>- Regulates cell apoptosis and growth factors                                   |
| Lin <i>et al</i> (26)              | 2013 | - Increases the synthesis of IFN- $\gamma$ and IL-17A by T-cells and suppresses apoptosis via programmed cell death protein 4 (PDCD4)<br>- Is responsible for sustaining the effector phase in effector T-cells |
| Piket <i>et al</i> (27)            | 2019 | - Up-regulated during active MS disease   |
| Tufekci <i>et al</i> (28)          | 2011 | - Upregulated after the activation of TLR4, myeloid cells, and macrophage<br>- Inhibition in the expression of IL12a, PTEN, and PDCD4<br>- Positive regulator of Foxp3 expression                               |
| Sheedy <i>et al</i> (29)           | 2015 | - miR-21 in T-cell may also play an important role in self-tolerance regulation<br>- Intrinsic miR-21 can also affect T-cell polarization   |
| Fenoglio <i>et al</i> (30)         | 2011 | - Significantly increased expression of miR-21 in relapsing-remitting (RR) MS patients<br>- Activation of CD4+ lymphocytes  |
| Muñoz-San Martín <i>et al</i> (12) | 2019 | - Overexpressed in the CSF of Gd+ and PBMCs of relapsing-remitting MS patients<br>- Associated with clinical disability   |

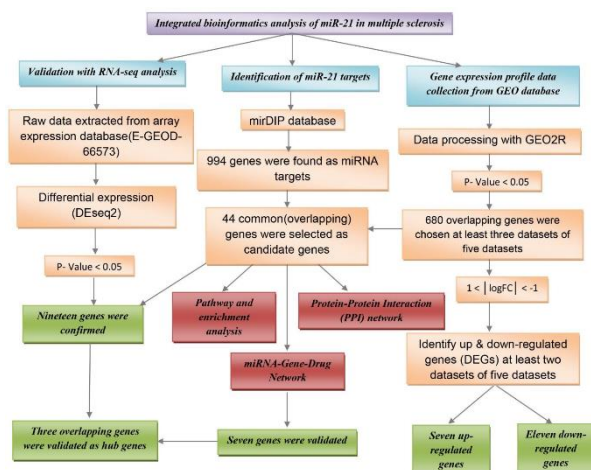


Figure 1. The bioinformatics flowchart used in the current study. DEGs: differentially expressed genes, PPI: protein-protein interaction, GEO: gene expression omnibus.

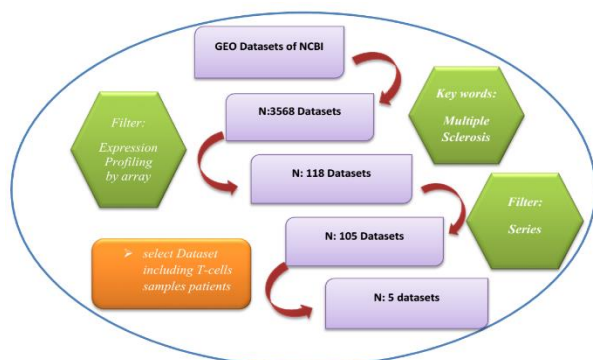


Figure 2. Outline of the protocol used for the search of multiple sclerosis microarray datasets from the GEO database.

pression profiling by array) were selected as keywords for the search in the GEO database. Finally, data were obtained from 5 mRNA microarrays (GSE43592, GSE13732, GSE16461, GSE78244, and GSE81279). The overall analysis process for this study is shown in figure 1 and the frame used for the selection of these datasets is shown in figure 2. The selected datasets included gene expression profiling using microarray in T-cells of patients with MS but datasets in which pa-

tients underwent treatment were excluded (Table 2).  $p < 0.05$  was set to determine significant expression changes. The study was expanded by adding *in-silico* predicted miRNAs based on available MS-related genes and pathways.

**Data preprocessing and analyzing of microarray**

The GEO2R interactive web tool (<https://www.ncbi.nlm.nih.gov/geo/info/geo2r.html>), using the GEO query and limma R packages, was applied for the analysis and comparison of the expression profiles of MS samples with controls in order to identify significant differences in gene expression after GEO2R analysis and obtain a final list of significant genes based on  $p < 0.05$  (Cut off). The final results of the analysis of DEGs for up- and down-regulated genes were obtained by using cut off values for  $p < 0.05$  and log Fold Change (logFC)  $> 1$  or  $\log FC < -1$ . According to this novel approach of combining microarray analysis and bioinformatics tools, common differentially expressed genes were identified and selected between the predicted targets of miR-21 and microarray datasets using a Venn diagram for showing T-cells from patients with MS. To investigate the potential role of miR-21 in gene regulation in MS, publically available microarray datasets containing non-coding RNA of peripheral blood profiles of controls and patients were downloaded which corresponded to platform specifications of GEO database<sup>31</sup>. Studies in which patients were receiving therapy or in which samples were not obtained from blood, were excluded. At least seven replicates of the examined GSE31568 dataset containing each miRNA were measured, and the median of the replica was computed. To process the collected data more specifically, experimentally validated targets of miR-21 were searched and used to construct a primary miRNA-mRNA-drug regulatory network.

**Prediction of miRNA target genes**

The predicted targets of miR-21 were obtained from the online functional annotation tool, mirDIP 4.1 (<http://ophid.utoronto.ca/mirDIP/>), which provides 152 million human microRNA-target predictions, collected across 28 different resources (BCmicrO, BiTargeting, CoMeTa, Cupid, DIANA, EIMMo3, GenMir++, MicroRNA.org, miRBase, mirCoX, miRcode, miRDB, miRTar2GO, MAMI, MBStar, MirAncesTar, Mir-

Table 2. Characteristics of the five gene expression profiling datasets for multiple sclerosis in integrated bioinformatics analysis

| GEO datasets    | Data       | Platform | Controls | MS patients | Tissue                 | Reference |
|-----------------|------------|----------|----------|-------------|------------------------|-----------|
| <b>MicroRNA</b> |            |          |          |             |                        |           |
| GSE31568        | Normalized | GPL9040  | 23       | 70          | Peripheral blood cells | (31)      |
| <b>Genes</b>    |            |          |          |             |                        |           |
| GSE78244        | Normalized | GPL17077 | 14       | 14          | CD4+T cells            | (32)      |
| GSE13732        | Raw        | GPL570   | 37       | 28          | CD4+T cells            | (33)      |
| GSE43591        | Normalized | GPL570   | 10       | 10          | T cells                | (34)      |
| GSE16461        | Normalized | GPL1707  | 8        | 8           | T cells                | (35)      |
| GSE81279        | Raw        | GPL21847 | 20       | 7           | T cells                | (36)      |

MAP, MirSNP, MirTar, Mirza-G, MultiMiTar, PAC-CMIT, PicTar, PITA, RepTar, RNA22, RNAhybrid, TargetRank, TargetScan, and TargetSpy)<sup>37</sup>. Then, the target genes were aligned with the DEGs in MS, and this was used for further analysis.

**Independent validation by RNA-sequencing (RNA-seq)**

Independent validation of the 44 common genes as candidate key genes was derived by integrated microarray analysis results and miRNA targets and independent samples of MS and healthy controls from RNA-seq experiment (GEO accession no. of GSE 94266) were selected. The original experiment was designed to determine the Differentially Expressed Genes (DEGs) in MS patient versus healthy controls. Quality control of reads was analyzed using FastQC package (<https://www.bioinformatics.babraham.ac.uk/projects/fastqc/>). Low quality reads and adaptor sequences were trim-med by the CLC Genomics Workbench 12.0.3 (QIAGEN, Germany). Mapping of short reads to the reference genome was performed using the CLC Genomics Workbench. Raw counts were obtained and used for Differential Expression (DE) analysis. The differential expression analysis was performed using DESeq2 and genes with  $p \leq 0.05$  were defined as Differentially Expressed Genes (DEGs).

**Functional and pathway enrichment analysis**

The Gene Ontology (GO) enrichment analysis including Biological Process (BP), Molecular Function (MF), and cellular component (CC), and the Kyoto encyclopedia of genes and genomes (KEGG) pathway enrichment analyses of common genes were carried out using the Enrichr database, which is a bioinformatics data platform consisting of an extensive biology knowledge database and analysis tools to align and explore significant biological information from large quantities of genes and protein collections<sup>38</sup>. A  $p < 0.05$  was used as the cut off criterion to determine the important pathways in which the genes are involved.

**PPI network construction**

The STRING (Search tool for the retrieval of interacting genes) database (<http://string-db.org/>) was used for constructing common DEGs network by calculating the protein-protein interaction.

**Prediction of drug-gene interaction**

Drugs and their target genes were downloaded from the drug-gene interaction database (DGIdb v3.0, [www.dgldb.org](http://www.dgldb.org))<sup>39,40</sup>. DGIdb normalizes content from 30 different sources and provides access through an intuitive web user interface, Application Programming Interface (API), and public cloud-based server image<sup>40</sup>. In addition, Cytoscape software was applied to extend gene-drug interaction network.

**miRNA- mRNA-drug interaction network**

mRNA-miRNA and drug-based disease-associated regulatory network were assessed by using microarray datasets in order to identify the relationship between

miR-21, differentially expressed genes, and well-known drugs in MS. To create networks between miRNA-genes and drugs, common genes between DEGs and predicted miR-21 targets and related drugs were selected to obtain the intersection for creating networks using Cytoscape software (<https://cytoscape.org/>).

**Results**

**Verification of miR-21 in MS**

In order to develop a miRNA gene-based disease-associated network, data were collected by three different methods to identify miRNAs associated with MS. MiR-21 was selected as a candidate biomarker in MS, based on previous findings regarding the role of miR-21 in gene regulation in the etiology of MS. There was a statistically significant increase in expression of miR-21 in the peripheral mononuclear cells of patients with Relapsing-Remitting (RR) MS compared to controls. For in silico analysis, the GSE31568 dataset contained 23 MS samples and 70 control samples and based on GPL9040 platform (febit Homo Sapiens miRBase 13.0), there was significantly up- and down-regulated miR-21 in peripheral blood cells (Table 3).

**Identification of differentially expressed genes (DEGs) in MS patients**

The five selected datasets were downloaded directly from GEO (<https://www.ncbi.nlm.nih.gov/geo/>) database and analyzed using GEO2R. They were identified as 7502, 14776, 1840, 3927, 140 DEGs in GSE43591, GSE13732, GSE16461, GSE78244, and GSE81279 and composed of up-and down-regulated expression based on criteria of log fold change  $> 1$  or  $< -1$  and  $p < 0.05$  in MS as described in table 3 and figure 3. Genes of datasets that were differentially expressed in the same gene symbol or overlapping gene, at least two of the five datasets, were selected (Figure 3). In total, 680 genes were obtained based on criteria of  $p < 0.05$  for carrying out the process analysis. Based on this novel approach, 44 genes (Table S1) were identified that overlapped as differentially expressed genes between the predicted target of miR-21 (994 genes) and microarray datasets (680 genes) using a Venn diagram (Table S2, Figure 4).

**Identification of predicted target genes for miR-21**

In this study, 994 predicted genes as potential target

Table 3. Microarray profiling for differential gene expression in T-cells of MS patients

| GSE datasets | p<0.05 significant genes | Up-regulated genes | Down-regulated genes |
|--------------|--------------------------|--------------------|----------------------|
| GSE43591     | 7502                     | 11                 | 12                   |
| GSE13732     | 14776                    | 25                 | 280                  |
| GSE16461     | 1840                     | 394                | 1159                 |
| GSE78244     | 3927                     | 154                | 37                   |
| GSE81279     | 140                      | 6                  | 5                    |

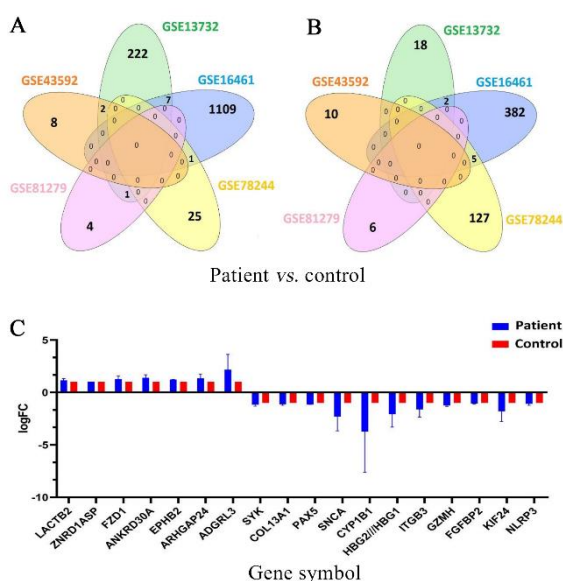


Figure 3. A) Venn diagram represents the number of overlapping differentially down-regulated genes between datasets based on  $|\text{Log FC}| < -1$  and  $p < 0.05$ . Eleven overlapping genes, at least two datasets, were shown. B) Venn diagram represents the number of overlapping differentially up-regulated genes between datasets based on  $|\text{Log FC}| > 1$  and  $p < 0.05$ . Seven overlapping genes, at least two datasets, were shown. C) differentially up- and down-regulated genes between datasets in MS patients versus healthy controls.

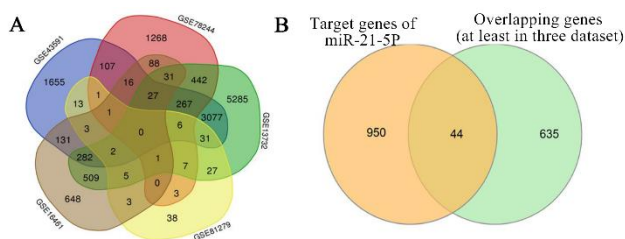


Figure 4. A) 680 overlapping genes, at least three of the five GEO datasets, by Venn diagram with  $p < 0.05$ . B) The common DEGs (44 genes) as overlapping genes of the predicted target genes of miR-21, at least three of five datasets, using process analysis demonstrated by Venn diagram. miR: microRNA, DEGs: differentially expressed genes, MS: multiple sclerosis.

genes of miR-21 were obtained by using mirDIP. All genes shown in table S1 were predicted by mirDIP as targets of miR-21. Then, the target genes were aligned with the DEGs in MS, and this was used for further analysis.

**RNA sequence analysis**

Our analysis identified 6332 mRNAs that were significantly differentially expressed between MS and healthy subjects ( $p < 0.05$ ), defined as differentially expressed genes. Then, overlapping genes between these genes and significant genes (44 common genes) and 18 mRNAs ( $p < 0.05$ ,  $1 < |\text{LogFC}| < -1$ ) were shown by microarray analysis (Figure 5).

[KDM7A- ATXN3- SNX13- SMC1A- TMEM106B- WSB1- PIKFYVE- DNAJC16- CAMSAP2- TNFAIP3- ETNK1- IRAK1BP1- RBMS1- U2SURP- ZADH2- NRIP1- RTKN2- BRWD1- AND S100A10]

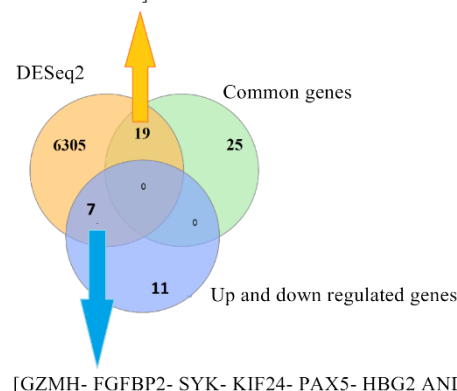


Figure 5. Venn diagram represents the number of overlapping differentially expressed genes between significant genes ( $n=6332$ ) of RNA-seq analysis, 44 common genes and 18 up- and down-regulated genes in multiple sclerosis disease. Validation of microarray result by RNA-seq showed 19 and 7 overlapping genes with common genes and up- and down-regulated genes, respectively.

**GO and KEGG pathway enrichment analyses of common genes**

GO and KEGG pathway enrichment analyses were performed for further investigation of the functional role of common DEGs and key pathways in MS patients. First of all, all common DEGs which had been submitted to the Enrichr online database were analyzed.

As shown in table 4, signaling pathway analysis was performed using KEGG analysis for all common DEGs (44 genes). The results of KEGG enrichment analysis showed that the common DEGs were mainly enriched in inositol phosphate metabolism, sulfur metabolism, phosphatidylinositol signaling system, HIF-1 signaling pathway, Th17 cell differentiation, and thiamine metabolism. For Cellular Component (CC), results of the top five GO terms (Table 5) reveal that 44 common DEGs were significantly enriched at microtubule minus-end, nuclear periphery, microtubule end, mitotic spindle pole, and membrane raft-mediated pathway (Table S3). For Biological Processes (BP), results of the top five GO enrichment analyses (Table 6) show

Table 4. Significantly enriched KEGG signaling pathways of the differentially expressed genes identified in multiple sclerosis

| KEGG pathway                          | p-value     | Genes           |
|---------------------------------------|-------------|-----------------|
| Inositol phosphate metabolism         | 0.011556016 | PIKFYVE; IMPAD1 |
| Sulfur metabolism                     | 0.019630393 | IMPAD1          |
| Phosphatidylinositol signaling system | 0.020048578 | PIKFYVE; IMPAD1 |
| HIF-1 signaling pathway               | 0.020429484 | ARNT; IL6R      |
| Th17 cell differentiation             | 0.023180005 | IL6R; TGFB2     |
| Thiamine metabolism                   | 0.032507623 | AK2             |

Table 5. Ten top GO enrichment analyses of 44 common differentially expressed genes (DEGs) with p<0.05

| Cellular component pathway ID        | p-value     | Genes   |
|--------------------------------------|-------------|---|
| Microtubule minus-end (GO:0036449)   | 1/31E-04    | <i>NIN; CAMSAP2</i>                           |
| Nuclear periphery (GO:0034399)       | 6/74E-04    | <i>ATF7; SMC1A; DCAF7</i>                     |
| Microtubule end (GO:1990752)         | 0/001062505 | <i>NIN; CAMSAP2</i>                           |
| Mitotic spindle pole (GO:0097431)    | 0/001374107 | <i>NIN; SMC1A</i>                             |
| Membrane raft (GO:0045121)           | 0/002276993 | <i>PIKFYVE; S100A10; TGFBR2</i>               |
| Nucleolus (GO:0005730)               | 0/00344751  | <i>ATXN3; NIN; NRIP1; WDFY3; BRWD1; KDM7A</i> |
| Caveola (GO:0005901)                 | 0/006755543 | <i>ATP2B4; TGFBR2</i>                         |
| Nuclear matrix (GO:0016363)          | 0/007474434 | <i>SMC1A; DCAF7</i>                           |
| Nucleoplasm part (GO:0044451)        | 0/012080201 | <i>PHF20; IMPAD1; ARNT; DCAF7</i>             |
| Gamma-secretase complex (GO:0070765) | 0/013129125 | <i>TMED10</i>                                 |

Table 6. Ten top biological process enrichment analyses of 44 common differentially expressed genes (DEGs) with p<0.05

| Biological process pathway ID  | p-value     | Genes                        |
|--|-------------|------------------------------|
| Protein K63-linked deubiquitination (GO:0070536)   | 3/13E-05    | <i>ATXN3; TNFAIP3; BRCC3</i> |
| Negative regulation of protein depolymerization (GO:1901880)   | 8/76E-04    | <i>LIMA1; CAMSAP2</i>        |
| Protein K48-linked deubiquitination (GO:0071108)   | 0/001162071 | <i>ATXN3; TNFAIP3</i>        |
| Cellular response to interleukin-6 (GO:0071354)  | 0/001162071 | <i>ST3GAL6; IL6R</i>         |
| Regulation of interleukin-6 production (GO:0032675)  | 0/003851281 | <i>TNFAIP3; IL6R</i>         |
| Regulation of smooth muscle cell proliferation (GO:0048660)  | 0/004219716 | <i>TNFAIP3; IL6R</i>         |
| Negative regulation of supramolecular fiber organization (GO:1902904)  | 0/006294875 | <i>LIMA1; CAMSAP2</i>        |
| Hemopoiesis (GO:0030097)   | 0/01215973  | <i>RTKN2; TGFBR2</i>         |
| Monoubiquitinated protein deubiquitination (GO:0035520)  | 0/013129125 | <i>ATXN3</i>                 |
| Regulation of epithelial to mesenchymal transition<br>Involved in endocardial cushion formation (GO:1905005) | 0/013129125 | <i>TGFBR2</i>                |

that they were significantly enriched and contained protein K63-linked deubiquitination, negative regulation of protein depolymerization, protein K48-linked deubiquitination, cellular response to interleukin-6, and regulation of interleukin-6 production (Table S4). In addition, according to the results of the top five GO analyses shown in table 7, 44 common DEGs were significantly enriched in Molecular Function (MF), including Lys63-specific deubiquitinase activity, ubiquitin-like protein-specific protease activity, thiol-dependent ubiquitin-specific protease activity, thiol-dependent ubiquitin hydrolase activity, and polyubiquitin modification-dependent protein binding (Table S5).

**Construction of protein-protein interaction network**

To assess the protein-protein interaction network, all DEGs were submitted to STRING. As shown in figure 6, PPI network analysis introduced 44 nodes and 6 edges for the common DEGs based on the PPI network modules and PPI enrichment with p-value of 0.638.

**Recognition of drugs related to common DEGs**

Next, an analysis of all the common DEGs using DGIdb v3.0 was carried out to detect affected genes associated with drugs in MS. An in-depth dissection of the effects of drugs on genes in MS was developed. These results demonstrated that seven genes in MS were targeted by drugs. According to table 8, multiple

Table 7. Ten top molecular functions enrichment analyses of 44 common differentially expressed genes (DEGs) with p<0.05

| Molecular function pathway ID  | p-value     | Genes                        |
|--|-------------|------------------------------|
| Lys63-specific deubiquitinase activity (GO:0061578)                      | 1/62E-06    | <i>ATXN3; TNFAIP3; BRCC3</i> |
| Ubiquitin-like protein-specific protease activity (GO:0019783)           | 5/77E-04    | <i>ATXN3; TNFAIP3; BRCC3</i> |
| Thiol-dependent ubiquitin-specific protease activity (GO:0004843)        | 6/24E-04    | <i>ATXN3; TNFAIP3; BRCC3</i> |
| Thiol-dependent ubiquitinyl hydrolase activity (GO:0036459)              | 0/001088282 | <i>ATXN3; TNFAIP3; BRCC3</i> |
| Polyubiquitin modification-dependent protein binding (GO:0031593)        | 0/004033525 | <i>TNFAIP3; BRCC3</i>        |
| Protein phosphatase 2B binding (GO:0030346)                              | 0/013129125 | <i>ATP2B4</i>                |
| Transforming growth factor beta-activated receptor activity (GO:0005024) | 0/013129125 | <i>TGFBR2</i>                |
| 1-phosphatidylinositol-4-phosphate 5-kinase activity (GO:0016308)        | 0/013129125 | <i>PIKFYVE</i>               |
| Interleukin-6 receptor binding (GO:0005138)                              | 0/015300881 | <i>IL6R</i>                  |
| Adenylate kinase activity (GO:0004017)                                   | 0/015300881 | <i>AK2</i>                   |

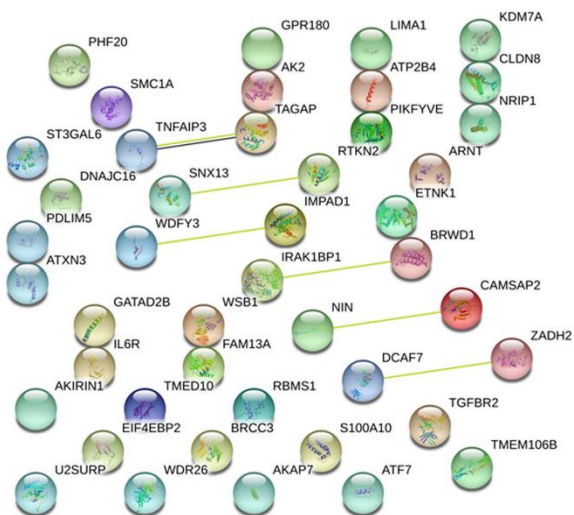


Figure 6. Protein-protein interaction of 44 common differentially expressed genes (DEGs) identified in multiple sclerosis by STRING.

drugs have regulatory and inhibitory roles in MS patients' genes.

**Construction of regulatory miRNA-mRNA-drug network**

This approach was eventually used to develop a miRNA-mRNA-drug interaction network and identify key genes co-regulated by miR-21-5p and drugs. To illustrate the complex correlation between drugs and gene targets of miR-21, a layered network using Cytoscape v3.6.1 was created that can provide more detailed information regarding these relationships. By integrated analyses, it was shown that 7 genes (*NRIP1*, *ARNT*, *KDM7A*, *S100A10*, *AK2*, *TGFBR2*, and *IL-6R*)

were regulated by obtained drugs and miR-21; in fact, miR-21 and drugs can synergistically regulate pathways in MS disease by regulating these genes (Figure 7).

**Discussion**

The involvement, functions, and complexity of miRNAs in autoimmune diseases are still unclear, especially in MS, due to the inadequate number of microarray expression profiles in MS studies<sup>19</sup>. Overexpression of miR-21 in patients with MS may be a signature in regulating genes and enhanced expression of pro-inflammatory factors such as IFN $\gamma$  and TNF- $\alpha$  after TCR stimulation. Up-regulation of miR-21 has been found in autoimmune diseases like IBD (Inflammatory Bowel Disease), SLE (Systemic Lupus Erythematosus), and psoriasis. Our findings suggest that miR-21 could be a target in clinical treatment for the inflamma-

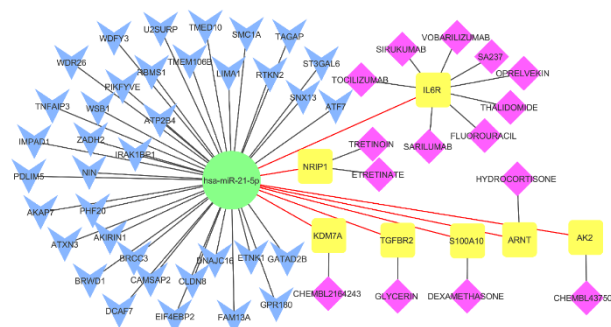


Figure 7. miRNA-mRNA-drug interaction network constructed by Cytoscape; miR-21 regulates common DEGs and is related with genes affected by MS-associated drugs. Blue: common DEGs, Yellow: common DEGs affected by drugs, Pink: MS-associated drugs.

Table 8. Results of the analysis of common DEGs in MS and targeted drugs using DGIdb v3.0

| Drug           | Interaction type    | Gene           | Sources  | PMIDs                        | Score |
|----------------|---------------------|----------------|--|------------------------------|-------|
| ChEMBL 2164243 | Inhibitor           | <i>KDM7A</i>   | Guide to Pharmacology  | None found                   | 1     |
| Glycerin       | N/A                 | <i>TGFBR2</i>  | DrugBank   | 17139284, 17016423           | 3     |
| Dexamethasone  | N/A                 | <i>S100A10</i> | NCI  | 10358078                     | 2     |
| Tretinoin      | N/A                 | <i>NRIP1</i>   | NCI  | 15632153, 14581481           | 3     |
| Etretinate     | N/A                 | <i>NRIP1</i>   | NCI  | 15180561                     | 2     |
|                |                     |                | - My Cancer Genome TGD Clinical Trial<br>- Guide to Pharmacology |                              |       |
| Tocilizumab    | Antibody, inhibitor | <i>IL6R</i>    | - ChEMBL interactions TEND<br>- DrugBank<br>- TTD                | 16899109                     | 8     |
| Sarilumab      | Antagonist          | <i>IL6R</i>    | - ChEMBL interactions<br>- TTD                                   | None found                   | 2     |
| Thalidomide    | N/A                 | <i>IL6R</i>    | NCI  | 12515619                     | 2     |
| Fluorouracil   | N/A                 | <i>IL6R</i>    | NCI  | 8888499                      | 2     |
| Oprelvekin     | Agonist             | <i>IL6R</i>    | Guide to Pharmacology  | None found                   | 1     |
| Vobarilizumab  | Antibody            | <i>IL6R</i>    | Guide to Pharmacology  | None found                   | 1     |
| SA237          | Antagonist          | <i>IL6R</i>    | ChEMBL interactions  | None found                   | 1     |
| Sirukumab      | N/A                 | <i>IL6R</i>    | TDG Clinical Trial   | None found                   | 1     |
| Hydrocortisone | N/A                 | <i>ARNT</i>    | NCI  | 10048155                     | 2     |
| ChEMBL 437508  | N/A                 | <i>AK2</i>     | DrugBank   | 10592235, 17139284, 17016423 | 4     |

tory component of MS<sup>24</sup>. Also, previous experimental studies have documented that T-cells transfected with miR-21 secreted IFN- $\gamma$  and TNF- $\alpha$  by affecting promoter regions and have binding sites for several transcriptional factors such as AP-1, STAT-3, MyD88, and NF- $\kappa$ B<sup>29</sup>. MiR-21 directly inhibits the expression of PDCD4 that acts as a biomarker in pathogenic T-cell apoptosis and cell proliferation in human SLE. Overexpression of miR-21 can lead to up-regulation of multiple genes which cause inflammation via activation of pathways such as NF- $\kappa$ B and MAPK<sup>41</sup>. miR-21 indirectly regulates Foxp3 expression<sup>42</sup>. Induced miR-21, upon TCR activation, regulates several signaling pathways including ERK, AP-1 and AKT through negative feedback. Activation of these signaling pathways results in increased effector cells and decreases memory T-cell differentiation<sup>43</sup>. Since predicting promoter region of pri-miR-21 is complex<sup>29</sup> and the exact roles of miR-21 are undetermined in MS disease, targeting miR-21 seems to be useful in developing a treatment based on the new approach. In the present study, publicly available microarray databases were used to analyze significantly differentially expressed genes in MS patients and to identify molecular interactions between miR-21-mRNA and drugs for demonstrating biochemical mechanisms related to MS. Therefore, a miRNA and a gene-drug network was created. Our network is different from previous studies in the literature because it is based on specific microarray datasets of T-cells in MS and pathway genes related to drugs. Also, our study identified 44 significantly up- and down-regulated common genes that may reflect the pathology and progression of MS. In this study, 44 new DEGs were found in T-cell MS datasets with overlap between at least three out of five microarray datasets. In the present study, to identify 994 putative target genes of miR-21, miRDIP was used which contained 28 different resources of functional annotation datasets. In addition, to obtain a final list of significant DEGs in T-cells from patients with and without MS, an analysis of five different datasets was performed, which identified 679 MS-associated genes. Integrated analysis between predicted target genes of miR-21 and DEGs of datasets revealed 44 common DEGs as overlapping genes that were associated with the development and progression of MS disease. Our findings revealed 7 up-regulated and 15 down-regulated genes at the intersection of the 44 common DEGs with five datasets that might be targets of miR-21 for the therapeutic approach. Therefore, the detection of putative target genes of miR-21 might identify how this miRNA controls different cell signaling pathways and molecular mechanisms in MS disease. The results of GO annotation revealed that some genes, such as *ATXN3*, *IL6R*, *AK2*, *ARNT*, and *TGFBR2* are mutually and significantly effective between pathways related to MS disease. Also, the results of KEGG pathway enrichment analysis showed that the *IL6R*, *AK2*, *ARNT*, and *TGFBR2* were the most significant

genes in the HIF-1 signaling pathway, Th17 cell differentiation, and thiamine metabolism pathways. Also, previous *in vitro* and *ex vivo* experimental studies have revealed that human Th17 cells were associated with disease activity and downstream pathways in the pathogenesis of autoimmunity<sup>44</sup> and they play distinctive effector roles in MS patients<sup>45</sup>. In addition, new drugs that targeted TH17 pathway such as Secukinumab (Cosentyx), human IgG1 $\kappa$  monoclonal antibody against IL-17A, can help in monitoring the disease activity and their potential role in inhibiting Th17 cell differentiation as therapeutic targets in the treatment of autoimmunity disorders<sup>44</sup> is confirmed based on findings in Experimental Autoimmune Encephalomyelitis (EAE) (MS disease model), and discovery of the biology and function of Th17 in encephalitogenicity<sup>46</sup>. To discover the functions and roles of 44 common DEGs in MS disease, their correlation with MS-related drugs was assessed and regulatory and inhibitory effects of drugs on genes of MS patients were found. These results, based on the scoring criteria, can confirm the findings of GO and KEGG analysis that *IL6R*, *AK2*, *TGFBR2*, and *ARNT* genes are significantly effective in MS disease. These results indicate the potential therapeutic targets of DEGs in autoimmune MS disease. Through integrated analysis of both hybrid miRNA-mRNA drug network with the Cytoscape, this study identified a noticeable relation between miR-21 and genes, indicating that miR-21 could play pivotal roles in regulating pathways and phenotypes of MS. Interestingly, the regulation of *TGFBR2* by miR-21 has been demonstrated by Luo *et al* similar to our analysis<sup>24</sup>. Moreover, Meira *et al* have reported the significant down-regulation of *TGFBR2* expression in RRMS patients compared to healthy controls<sup>47</sup>. In our analysis, *ARNT* genes were mainly involved in MS disease pathways, whereas Zorlu *et al* showed that this gene is consistently associated with MS in patients at the secondary progressive phase of the disease<sup>48</sup>. *AK2* as a novel apoptotic pathway<sup>49</sup>, the pivotal role of the *AK2* gene in hematopoiesis, and its association with a pathway controlling cell growth and survival were all explained by previous research<sup>50</sup>. Although the exact role of *AK2*, *ARNT*, and *ATXN3* in MS disease has not been studied yet, they be candidate therapies for MS disease. However, the effect of miR-21 on *AK2*, *ATXN3*, and *ARNT* has not been studied in MS disease and requires further investigation. miRNA is an ideal candidate for therapeutic targets due to the role of miRNAs in controlling various gene expression in cancer and several other diseases, in particular autoimmune diseases<sup>51</sup>. Nineteen genes among common genes were validated with RNA sequencing in this study. Finally, three overlapping genes (*S100A10*, *NRIP1*, *KDM7A*) were identified between miRNA-gene-drug network and nineteen genes as hub genes that may reflect the pathology of MS. It has been found that *NRIP1* is involved in CNS-mediated neurophysiological processes and ad-



ministration of Toll like-receptor ligands affects inflammatory potential in macrophages through their function as co-activators for NF- $\kappa$ B<sup>52</sup>. He *et al* have mentioned that methylation is controlled by histone lysine methyltransferases (KMTs) and demethylases (KDMs) that possess strong substrate specificity and they have reported that histone lysine demethylases (KDMs) such as KMD7A play critical roles in the pathogenesis of MS<sup>53</sup>. It has been identified that S100A10 as the specific marker of A2 astrocytes is essential for cell proliferation, membrane repair, and inhibition of cell apoptosis. Astrocytes play a key role in demyelinating diseases, like multiple sclerosis<sup>54</sup>. Recent data demonstrate that artificial antisense miRNAs, such as Locked Nucleic Acid (LNA), bind to complementary RNA with high affinity and have stability and low toxicity without inducing the immune response<sup>55</sup>; therefore, they could be applied to block their targeted oncomiRs to prevent the development of cancer. Also, antisense miRNAs as a gene silencing factor could significantly affect the prognosis of the disease<sup>51</sup>. In particular, LNA against miR-122 represents an effective approach in the treatment of hepatitis C (Phase II trial)<sup>55</sup>.

### Conclusion

The computational approach used in this study demonstrated the role of miR-21 as a regulator of the MS-related signaling pathways which can be a potential target for therapeutic modalities. Based on complex miRNA-mRNA interactions, genes targeted by many miRNAs have several sites for the same miRNA. However, the findings of the current study should be confirmed with available techniques such as real-time PCR and western blotting or luciferase assay. Since experimental validation of miRNA targets with laboratory techniques is expensive and cumbersome, the results of current bioinformatic approach would be an effective method for guiding in vivo and in vitro experiments.

An integrated miRNA-mRNA-drug network was developed to analyze predicted MS-associated target genes of miR-21, followed by functional enrichment assessment of the miR-21 targeted DEGs in MS patients. Based on the crucial effect of miR-21 on genes in MS patients, our research suggests applying miR-21 inhibitors such as locked nucleic acid (LNA)-modified oligonucleotides that are known as stable, non-toxic drugs which do not induce an aberrant immune response<sup>56</sup>. Altogether, these findings can provide new insights into pathogenicity mechanisms of MS, therapeutic development, and interventions. Further studies are required to confirm the results of the present study in MS patients.

### Availability of data and materials

All data generated or analyzed during this study are included in this published article.

### Acknowledgement

This work was extracted from the Ph.D. thesis and financially supported by Vice Chancellor for Research Affairs of Iran University of Medical Sciences, Tehran, Iran through the registration No: 15.

### Conflict of Interest

The authors declare no conflict of interest.

### References

- Ramagopalan SV, Dobson R, Meier UC, Giovannoni G. Multiple sclerosis: risk factors, prodromes, and potential causal pathways. *Lancet Neurol* 2010;9(7):727-39.
- Sadeghian-Rizi T, Alsahebhosoul F, Kazemi M, Khanahmad H, Jahanian-Najafabadi A. Association of AIRE polymorphism and the susceptibility to multiple sclerosis in Iranian population. *Avicenna J Med Biotechnol* 2018; 10(2):110-4.
- Munoz-Culla M, Irizar H, Otaegui D. The genetics of multiple sclerosis: review of current and emerging candidates. *Appl Clin Genet* 2013;6:63-73.
- Australia and New Zealand Multiple Sclerosis Genetics Consortium (ANZgene). Genome-wide association study identifies new multiple sclerosis susceptibility loci on chromosomes 12 and 20. *Nat Genet* 2009;41(7):824-8.
- Didonna A, Oksenberg JR. Genetic determinants of risk and progression in multiple sclerosis. *Clin Chim Acta* 2015;449:16-22.
- Kim YA, Wuchty S, Przytycka TM. Identifying causal genes and dysregulated pathways in complex diseases. *PLoS Comput Biol* 2011;7(3):e1001095.
- Malkki H. Blood-based biomarkers provide insight into progressive MS. *Nat Rev Neurol* 2014;10(11):612.
- Raphael I, Webb J, Stuve O, Haskins W, Forsthuber T. Body fluid biomarkers in multiple sclerosis: how far we have come and how they could affect the clinic now and in the future. *Expert Rev Clin Immunol* 2015;11(1):69-91.
- Hosseini SM, Soltani BM, Tavallaei M, Mowla SJ, Tafsiiri E, Bagheri A, et al. Clinically significant dysregulation of hsa-miR-30d-5p and hsa-let-7b expression in patients with surgically resected Non-small cell lung cancer. *Avicenna J Med Biotechnol* 2018;10 (2):98-104.
- Soreq H, Wolf Y. NeurimmiRs: microRNAs in the neuroimmune interface. *Trends Mol Med* 2011;17(10): 548-55.
- Hendrickx DAE, van Scheppingen J, van der Poel M, Bossers K, Schuurman KG, van Eden CG, et al. Gene expression profiling of multiple sclerosis pathology identifies early patterns of demyelination surrounding chronic active lesions. *Front Immunol* 2017;8:1810.
- Muñoz-San Martín M, Reverter G, Robles-Cedeño R, Buxò M, Ortega FJ, Gómez I, et al. Analysis of miRNA signatures in CSF identifies upregulation of miR-21 and miR-146a/b in patients with multiple sclerosis and active lesions. *J Neuroinflammation* 2019;16(1):220.
- Bartel DP. MicroRNAs: genomics, biogenesis, mechanism, and function. *Cell* 2004;116(2):281-97.

14. Jernås M, Malmestrom C, Axelsson M, Nookaew I, Wadenvik H, Lycke J, et al. MicroRNA regulate immune pathways in T-cells in multiple sclerosis (MS). *BMC Immunol* 2013;14(1):32.
15. Li Z, Yu X, Shen J, Wu WK, Chan MT. MicroRNA expression and its clinical implications in Ewing's sarcoma. *Cell Prolif* 2015;48(1):1-6.
16. D'Ambrosio A, Pontecorvo S, Colasanti T, Zamboni S, Francia A, Margutti P. Peripheral blood biomarkers in multiple sclerosis. *Autoimmun Rev* 2015;14(12):1097-110.
17. Satoh JI, Tabunoki H, Yamamura T. Molecular network of the comprehensive multiple sclerosis brain-lesion proteome. *Mult Scler* 2009;15(5):531-41.
18. Freiesleben S, Hecker M, Zettl UK, Fuellen G, Taher L. Analysis of microRNA and gene expression profiles in multiple sclerosis: integrating interaction data to uncover regulatory mechanisms. *Sci Rep* 2016;6:34512.
19. Srinivasan S, Severa M, Rizzo F, Menon R, Brini E, Mechelli R, et al. Transcriptional dysregulation of interferome in experimental and human multiple sclerosis. *Sci Rep* 2017;7(1):8981.
20. Safari-Alighiarloo N, Rezaei-Tavirani M, Taghizadeh M, Tabatabaei SM, Namaki S. Network-based analysis of differentially expressed genes in cerebrospinal fluid (CSF) and blood reveals new candidate genes for multiple sclerosis. *PeerJ* 2016;4:e2775.
21. Rahman MR, Islam T, Gov E, Turanli B, Gulfidan G, Shahjaman M, et al. Identification of prognostic biomarker signatures and candidate drugs in colorectal cancer: nsights from systems biology analysis. *Medicina (Kaunas)* 2019;55(1):20.
22. Islam T, Rahman MR, Karim MR, Huq F, Quinn JMW, Moni MA. Detection of multiple sclerosis using blood and brain cells transcript profiles: Insights from comprehensive bioinformatics approach. *Informatics in Medicine Unlocked* 2019;16:100201.
23. Liu Y, Chen G, Liu H, Li Z, Yang Q, Gu X, et al. Integrated bioinformatics analysis of miRNA expression in Ewing sarcoma and potential regulatory effects of miR-21 via targeting ALCAM/CD166. *Artificial Cells* 2019;47(1):2114-22.
24. Luo D, Fu J. Identifying characteristic miRNAs-genes and risk pathways of multiple sclerosis based on bioinformatics analysis. *Oncotarget* 2018;9(4):5287-300.
25. Ma X, Zhou J, Zhong Y, Jiang L, Mu P, Li Y, et al. Expression, regulation and function of microRNAs in multiple sclerosis. *Int J Med Sci* 2014;11(8):810-8.
26. Lin Q, Geng Y, Zhao M, Lin S, Zhu Q, Tian Z. MiR-21 regulates TNF- $\alpha$ -induced CD40 expression via the SIRT1-NF- $\kappa$ B pathway in renal inner medullary collecting duct cells. *Cell Physiol Biochem* 2017;41(1):124-36.
27. Piket E, Zheleznyakova GY, Kular L, Jagodic M. Small non-coding RNAs as important players, biomarkers and therapeutic targets in multiple sclerosis: A comprehensive overview. *J Autoimmun* 2019;101:17-25.
28. Tufekci KU, Oner MG, Genc S, Genc K. MicroRNAs and Multiple Sclerosis. *Autoimmune Dis* 2011;2011: 807426.
29. Sheedy FJ. Turning 21: Induction of miR-21 as a key switch in the inflammatory response. *Front Immunol* 2015;6(19).
30. Fenoglio C, Cantoni C, De Riz M, Ridolfi E, Cortini F, Serpente M, et al. Expression and genetic analysis of miRNAs involved in CD4+ cell activation in patients with multiple sclerosis. *Neurosci Lett* 2011;504(1):9-12.
31. Keller A, Leidinger P, Bauer A, Elsharawy A, Haas J, Backes C, et al. Toward the blood-borne miRNome of human diseases. *Nat Methods* 2011;8(10):841-3.
32. Hellberg S, Eklund D, Gawel DR, Kopsen M, Zhang H, Nestor CE, et al. Dynamic response genes in CD4+ T cells reveal a network of interactive proteins that classifies disease activity in multiple sclerosis. *Cell Rep* 2016; 16(11):2928-39.
33. Corvol JC, Pelletier D, Henry RG, Caillier SJ, Wang J, Pappas D, et al. Abrogation of T cell quiescence characterizes patients at high risk for multiple sclerosis after the initial neurological event. *Proc Natl Acad Sci USA* 2008;105(33):11839-44.
34. Jernas M, Malmstrom C, Axelsson M, Nookaew I, Wadenvik H, Lycke J, et al. MicroRNA regulate immune pathways in T-cells in multiple sclerosis (MS). *BMC Immunol* 2013;14:32.
35. Annibali V, Ristori G, Angelini DF, Serafini B, Mechelli R, Cannoni S, et al. CD161(high)CD8+T cells bear pathogenetic potential in multiple sclerosis. *Brain* 2011; 134(Pt 2):542-54.
36. Jangi S, Gandhi R, Cox LM, Li N, von Glehn F, Yan R, et al. Alterations of the human gut microbiome in multiple sclerosis. *Nat Commu.* 2016;7:12015.
37. Tokar T, Pastrello C, Rossos AEM, Abovsky M, Hauschild AC, Tsay M, et al. mirDIP 4.1-integrative database of human microRNA target predictions. *Nucleic Acids Res* 2017;46(D1):D360-D70.
38. Mou T, Zhu D, Wei X, Li T, Zheng D, Pu J, et al. Identification and interaction analysis of key genes and microRNAs in hepatocellular carcinoma by bioinformatics analysis. *World J Surg Oncol* 2017;15(1):63.
39. Griffith M, Griffith OL, Coffman AC, Weible JV, Mc Michael JF, Spies NC, et al. DGIdb: mining the drug-gable genome. *Nat Methods* 2013;10(12):1209-10.
40. Cotto KC, Wagner AH, Feng Y-Y, Kiwala S, Coffman AC, Spies G, et al. DGIdb 3.0: a redesign and expansion of the drug-gene interaction database. *Nucleic Acids Res* 2017;46(D1):D1068-D73.
41. Ando Y, Yang GX, Kenny TP, Kawata K, Zhang W, Huang W, et al. Overexpression of microRNA-21 is associated with elevated pro-inflammatory cytokines in dominant-negative TGF-beta receptor type II mouse. *J Autoimmun* 2013;41:111-9.
42. Tufekci KU, Oner MG, Genc S, Genc K. MicroRNAs and multiple sclerosis. *Autoimmune Dis* 2010;2011: 807426-.
43. Kim C, Hu B, Jadhav RR, Jin J, Zhang H, Cavanagh MM, et al. Activation of miR-21-regulated pathways in immune aging selects against signatures characteristic of memory T cells. *Cell Rep* 2018;25(8):2148-62.e5.

44. Dos Passos GR, Sato DK, Becker J, Fujihara K. Th17 Cells pathways in multiple sclerosis and neuromyelitis optica spectrum disorders: pathophysiological and therapeutic implications. *Mediators Inflamm* 2016;2016: 5314541.
45. van Langelaar J, van der Vuurst de Vries RM, Janssen M, Wierenga-Wolf AF, Spilt IM, Siepmann TA, et al. T helper 17.1 cells associate with multiple sclerosis disease activity: perspectives for early intervention. *Brain* 2018; 141(5):1334-49.
46. Rostami A, Ciric B. Role of Th17 cells in the pathogenesis of CNS inflammatory demyelination. *J Neurol Sci* 2013;333(1-2):76-87.
47. Meira M, Sievers C, Hoffmann F, Rasenack M, Kuhle J, Derfuss T, et al. Unraveling natalizumab effects on deregulated miR-17 expression in CD4+ T cells of patients with relapsing-remitting multiple sclerosis. *J Immunol Res* 2014;2014:897249.
48. Zorlu N, Hoffjan S, Haghikia A, Deyneko IV, Epplen JT. Evaluation of variation in genes of the arylhydrocarbon receptor pathway for an association with multiple sclerosis. *J Neuroimmunol* 2019;334:576979.
49. Lee HJ, Pyo JO, Oh Y, Kim HJ, Hong SH, Jeon YJ, et al. AK2 activates a novel apoptotic pathway through formation of a complex with FADD and caspase-10. *Nat Cell Biol* 2007;9(11):1303-10.
50. Lagresle-Peyrou C, Six EM, Picard C, Rieux-Laucat F, Michel V, Ditadi A, et al. Human adenylate kinase 2 deficiency causes a profound hematopoietic defect associated with sensorineural deafness. *Nat Genet* 2009;41(1):106-11.
51. Christopher A, Kaur R, Kaur G, Kaur A, Gupta V, Bansal P. MicroRNA therapeutics: Discovering novel targets and developing specific therapy. *Perspect Clin Res* 2016;7(2):68-74.
52. Flaisher-Grinberg S, Tsai HC, Feng X, Wei LN. Emotional regulatory function of receptor interacting protein 140 revealed in the ventromedial hypothalamus. *Brain Behav Immun* 2014;40:226-34.
53. He H, Hu Z, Xiao H, Zhou F, Yang B. The tale of histone modifications and its role in multiple sclerosis. *Hum Genomics* 2018;12(1):31.
54. Allnoch L, Baumgärtner W, Hansmann F. Impact of astrocyte depletion upon inflammation and demyelination in a murine animal model of multiple sclerosis. *Int J Mol Sci* 2019;20(16):3922.
55. Nedaeinia R, Sharifi M, Avan A, Kazemi M, Rafiee L, Ghayour-Mobarhan M, et al. Locked nucleic acid anti-miR-21 inhibits cell growth and invasive behaviors of a colorectal adenocarcinoma cell line: LNA-anti-miR as a novel approach. *Cancer Gene Ther* 2016;23(8):246-53.
56. Nedaeinia R, Avan A, Ahmadian M, Nia SN, Ranjbar M, Sharifi M, et al. Current status and perspectives regarding LNA-Anti-miR oligonucleotides and micro-RNA miR-21 inhibitors as a potential therapeutic option in treatment of colorectal cancer. *J Cell Biochem* 2017; 118(12):4129-40.

Supplementary

Table S1. 44 genes were identified that overlapped as differentially expressed genes between the predicted target of miR-21 and microarray datasets

| Gene symbol    | Gene symbol     | Gene symbol     | Gene symbol    |
|----------------|-----------------|-----------------|----------------|
| <i>GATAD2B</i> | <i>S100A10</i>  | <i>AKAP7</i>    | <i>BRCC3</i>   |
| <i>KDM7A</i>   | <i>RTKN2</i>    | <i>ATP2B4</i>   | <i>LIMA1</i>   |
| <i>TAGAP</i>   | <i>AKIRIN1</i>  | <i>IRAK1BP1</i> | <i>CLDN8</i>   |
| <i>FAM13A</i>  | <i>ETNK1</i>    | <i>SMC1A</i>    | <i>RBMS1</i>   |
| <i>ST3GAL6</i> | <i>EIF4EBP2</i> | <i>TMEM106B</i> | <i>SNX13</i>   |
| <i>TGFBR2</i>  | <i>WSB1</i>     | <i>IL6R</i>     | <i>ATF7</i>    |
| <i>PIKFYVE</i> | <i>NRIP1</i>    | <i>TMED10</i>   | <i>GPR180</i>  |
| <i>ZADH2</i>   | <i>DNAJC16</i>  | <i>PDLIM5</i>   | <i>U2SURP</i>  |
| <i>DCAF7</i>   | <i>WDR26</i>    | <i>BRWD1</i>    | <i>WDFY3</i>   |
| <i>TNFAIP3</i> | <i>NIN</i>      | <i>ATXN3</i>    | <i>CAMSAP2</i> |
| <i>PHF20</i>   | <i>IMPAD1</i>   | <i>ARNT</i>     | <i>AK2</i>     |

Table S2. 680 overlapping genes, at least three of the five GEO datasets, with p<0.05

| Gene symbol | Gene symbol | Gene symbol | Gene symbol | Gene symbol | Gene symbol | Gene symbol | Gene symbol           | Gene symbol        | Gene symbol                          | Gene symbol     | Gene symbol                    | Gene symbol | Gene symbol | Gene symbol |
|-------------|-------------|-------------|-------------|-------------|-------------|-------------|-----------------------|--------------------|--------------------------------------|-----------------|--------------------------------|-------------|-------------|-------------|
| CMKLR1      | EPB41L3     | PLBD1       | ARHGAP30    | PTBP3       | ELOVL5      | PIGS        | CTNNB1                | ITPK1-AS1          | KDSR                                 | BDP1            | ZDHHC14                        | RUFY2       | IFNGR1      |             |
| CYBB        | WSB1        | CDC73       | CENPO       | STAB1       | NOP9        | UBAP2L      | IFIH1                 | CCL28              | BCL2L14                              | IMPAD1          | SLC30A5                        | PDE4A       | HLA-DRB1    |             |
| CD44        | WDR26       | ITFG1       | MNDA        | SSR2        | FAM76B      | RPL23AP32   | TOLLIP                | UBE4B              | TAF5L                                | VPS16           | OFCC1                          | CYP11B      | CD5         |             |
| TRAF3       | FAM13A      | GAS7        | F11         | TPT1-AS1    | SEN7        | CD81        | TICAM1                | LYL1               | MAST2                                | GPLD1L          | LINC00487                      | BRWD1       | IL18        |             |
| TLR2        | NDE1        | LINC01578   | CTSS        | TRAF3IP3    | NDUFC1      | INPP5D      | INPP5D                | WDR5               | IKZF5                                | ADAMTS6         | ZC3H10                         | PANX1       | GPR180      | GPR180      |
| BCL10       | FCGR2A      | TIMP2       | LPCAT2      | DMWD        | ITPR1P2     | MS4A7       | RAF1                  | RANBP10            | GIMAP8                               | MKKS            | EIF3K                          | EIF3K       | ICAM4       |             |
| TRIM56      | MDC1        | SNX24       | LMO2        | TSPAN17     | FAM229A     | TBC1D10B    | ATG5                  | MCM3AP             | PHF3                                 | SLC25A30        | HPS5                           | TSC22D1-AS1 | HTRA1       |             |
| PITPNC1     | WDFY3       | MT1H        | CCDC134     | MT2A        | ZFP41       | GATAD2B     | ILF3                  | MFSD4B             | GPATCH2L                             | MIR6791//GPR108 | UBR2                           | SQSTM1      | GDF7        |             |
| LINC01210   | ZDHHC3      | FAM208A     | AK2         | FLT4        | VT1A        | XPO5        | INIP                  | UGP2               | PLXNC1                               | CDK13           | ARHGAP27                       | ZNF397      | SMAD6       |             |
| PPHLN1      | PSD4        | SRSF5       | SKIV2L      | RHBDD1      | CFAP44      | CCL2        | CMPK2                 | APOBEC3G           | C10orf76                             | RPS6KA4         | PDE12                          | ZNF148      | NFATC4      |             |
| EPHA3       | CAMSAP2     | TMEM106B    | RSBN1L      | ARHGFE10L   | DNAJC16     | ZNF160      | PHF20                 | UCHL5              | RPS2P45                              | LOC100102903    | LOC100996385                   | CNOT4       | ABCC3       |             |
| BAZZA       | FUT11       | MS4A14      | FAM131A     | TNIK        | HMOX1       | KLC2        | QKI                   | COX4I1             | LOC101929219//LOC100505650//C1orf186 | DOCK9-AS2       | CEP250                         | IKZF1       | SLC6A15     |             |
| EXOSC2      | FBXL17      | RTKN2       | AARS2       | TPP2        | IP6K2       | PART1       | DCUN1D5               | LOC145783//ZNF280D | TRMT44                               | CD247           | FBXO42                         | BRMS1       | TPMT        |             |
| ACOX1       | ATP2B4      | U2SURP      | SRPK2       | ZSCAN30     | EIF5B       | SAMD1       | NFYC                  | MAP4K4             | GUSBP11                              | SFT2D3//WDR33   | ARNT                           | ARNT        | LINC00960   |             |
| ZNF41       | ILDR1       | PIKFYVE     | STK4        | FAM13A-AS1  | FLCN        | MST1        | ZSCAN12               | WNKI               | C20orf196                            | CLCN3           | CLCC1                          | BTRC        | PEX26       |             |
| FGFR2       | SLC7A7      | HNMT        | TGOLN2      | CCDC141     | DMXL2       | POLQ        | MCFL2                 | WAC                | ER12                                 | POLR2A          | CDC14A                         | MAU2        | BRD2        |             |
| LOC283788   | CA5B        | NECTIN2     | ATP6V1G1    | CSTF3       | CSGALNACT1  | CLDN8       | ZNF775                | LRIG2              | PML                                  | SLC35C1         | SSTR2                          | PPP2R1B     | TCOF1       |             |
| FZD1        | FRG1BP      | ALDH2       | SNX3        | COPA        | TRNT1       | EPHB2       | F2RL2                 | VPS33A             | BPTF                                 | RNH1            | MIR6824//SLC26A6               | FAM208B     | PDLIM5      |             |
| ETNK1       | CSNK2A1     | SBN02       | RAB5C       | USP10       | ARSD        | ZDHHC8      | ELP6                  | TOP3A              | MGA                                  | CCDC71L         | LOC101930655//C7orf73//SLC13A4 | CEP162      | AKAP7       |             |
| SLC8A1      | SAT1        | RAB35       | THUMPDI     | LY86        | TMED10      | MICAL3      | CANT1                 | BETIL              | FLT3                                 | KIR3DL3         | SORT1                          | ARL10       | HIF3A       |             |
| PREP        | RBMS1       | FKRP        | IRGQ        | CCDC102A    | SEC62       | ATF7        | LOC339803             | FRY                | MMAA                                 | OVOL1           | LOC101929964//LINC01184        | NEU3        | DST         |             |
| SNX25       | TSPAN32     | APPBP2      | BCPIP       | RET         | TP53        | PAK4        | TRPM3                 | BIRC5              | HNRNPM                               | ZNF2            | KIR2DL4                        | TBKBP1      | CCNB1       |             |
| RAP1A       | NID1        | CST3        | RNASET2     | MID1        | AZ12        | PURG        | FAF8                  | EIF3M              | TRIM44                               | GAK             | CELF1                          | P2RY12      | NRXN1       |             |
| CD163       | HCP5        | OPA1        | CCND2       | LRRC25      | INSIG1      | TAB1        | SNRPB2                | POM121L12          | SLC45A4                              | PAX5            | DYNC1H1                        | PYHIN1      | P2RY2       |             |
| TBL1X       | RAB14       | VSTM4       | ATP5C1      | MS4A6A      | L3MBTL1     | LMX1A       | PMS1                  | TLL11              | MTMR2                                | OSER1-AS1       | ADGRG5                         | WDR78       | SYK         |             |
| LOC10192704 | DYNC1L12    | ZNF107      | TTPAL       | ATXN3       | SOS1        | CTNNA3      | RAB28                 | DIDO1              | IL16                                 | ZNF641          | BCAP29                         | MOGAT2      | SOC52       |             |
| ABI2        | SMCJA       | CNO77       | BCAT1       | CDC42       | PACSIN2     | CXCR4       | GSE1                  | CARS               | TTN                                  | MYO10           | IQSEC2                         | DOT1L       | PKHD1       |             |
| VPS53       | FCGR1B      | CTSK        | LIG3        | PER3        | BTG1        | GF11        | AP2A2                 | IL27RA             | TARP                                 | DLG3            | NEK6                           | SEMA6A      | SGCD        |             |
| RBM14       | RRAS2       | DHCR7       | TAOK1       | CCNT2       | CDKN1B      | ALAS1       | ABTB1                 | SEN8               | NDUFA10                              | ARIH2           | PSMD6-AS2                      | ATRIP//TRX1 | LAMB2       |             |
| TUBA1B      | ARPC5       | TMEM259     | GNL3        | AIF1        | DNAH6       | POLR1B      | KMT2C                 | ARFGFE2            | LRCH3                                | AP2A1           | BRCC3                          | ISTNA1      | STEAP3      |             |
| MROH2B      | ANXA6       | TEPSIN      | MON1B       | ARHGGEF40   | RHRP1       | MAF         | TMEM110               | ZNF781             | TTC9                                 | PLEKHG3         | KCND3                          | PPP1R12B    | KIF5A       |             |
| RANBP3      | BRE-AS1     | ZNF862      | ANAPC4      | TYW3        | DNAJC3      | CXCL1       | ZADH2                 | EXOSC3             | ABHD6                                | GLB1L2          | LRRC42                         | BACE1       | MEGF8       |             |
| ZNF322      | ST3GAL6     | HN1L        | TMX4        | DDIT4       | LIMA1       | TNF         | EIF4EBP2              | LOC389834          | PRKCA                                | PDGFB           | SNX13                          | NUP188      | COR06       |             |
| JAK3        | SEPT9       | HNRNPA2B1   | KIAA1033    | FAM198B     | SIRPB1      | XCL1        | MIR146A               | LIMS1              | RDH10                                | LRPPRC          | TMEM185B                       | NIN         | ATP5SL      |             |
| NCR1        | TCEB3       | CLEC7A      | AGTPBP1     | S1PR1       | MPP1        | LCK         | LOC149684//BPI        | SLC25A42           | PTCD3                                | ZBTB7A          | UBE2L3                         | ZKSCAN5     | SPIRE1      |             |
| C1R         | SLC26A11    | VPS37A      | BRD4        | PPME1       | GFM1        | BCL2L11     | PTGDR                 | KIAA1109           | CTAGE5                               | DCAF7           | LCMT2                          | PRB1        | CCDC171     |             |
| CCN1        | MARCH7      | PHACTR2     | TNRC18      | ACAD10      | DIS3L2      | TNFSF13B    | CDK12                 | IRAK1BP1           | FAM129C                              | RIMKL3          | FAM120AOS                      | VPS18       | ABLIM3      |             |
| OSBPL8      | MTIX        | MAFB        | CPVL        | S100A10     | TMEM41B     | CEBPB       | MTF1                  | C5orf63            | FOXK2                                | ACPP            | NLRX1                          | ATP8A1      | TGFBR2      |             |
| NR4A2       | NUP50       | AKR1C1      | TRAM2       | UBQLN1      | NFAM1       | IRAK4       | LINC00894             | ZNF717             | ING5                                 | ZNRF2           | B3GALT2                        | MRPS27      | SERPING1    |             |
| AP1S2       | S100A8      | GABBR2      | LOC153684   | POLR2C      | MLX         | IL6R        | NFKBID                | RNF216             | POLR2J4                              | SCARB1          | KIDINS220                      | UBTD2       | CD74        |             |
| CDK1        | TRAPPC10    | IGF2R       | PPCDC       | DERL1       | TAX1BP1     | TAGAP       | OXR1                  | IKBK3              | SPTBN1                               | HACD3           | DDX31                          | AKAP13      | TIRAP       |             |
| SETDB1      | RAP2B       | FCER1G      | SULF2       | RASGRF2     | FAM35A      | TNFAIP3     | NAGS                  | ST6GALNAC4         | MED27                                | CIC             | DNAJC21                        | EFCA1B3     | HFE         |             |
| SAMSN1      | HMG2        | APEX2       | PIEL        | CSF1R       | C11orf21    | CXCL2       | KEAP1                 | CNIH4              | NCAM1                                | HTT             | DNM2                           | SSX2IP      |             |             |
| SEC14L1     | PPP1R2      | PFKFB4      | KMT2B       | TMF1        | COTL1       | IFNAR2      | GLS                   | GPATCH2            | TPGS2                                | IFT27           | PDZD4                          |             |             |             |
| KLF4        | LRIF1       | SREBF1      | PPARD       | CRTAM       | MARCKS      | CD59        | PTPN1                 | DCAF10             | NFYA                                 | MRPS5           | ZFAND5                         | TMED1       |             |             |
| AKIRIN1     | MED17       | PWWP2B      | STK10       | MTF         | VCPKMT      | RELA        | LINC00528             | C9orf40            | MAGOHB                               | STRBP           | RNF8                           | JAK2        |             |             |
| ANKRD26     | SPOCK2      | CN2M2       | ZFAND1      | LILRB2      | NPEPPS      | CD48        | NTP160                | VRK3               | SVIL                                 | PLAGL2          | BAALC-AS2                      | CASP2       |             |             |
| B2M         | DIAPH1      | ERCC6L2     | KDM7A       | SLC33A1     | CREG1       | CD40LG      | LOC101928589//TMEM164 | TMTC1              | TLK1                                 | HNF4A           | ZNF91                          | LTB4R       |             |             |
| SEPHS1      | GTF3C4      | RAB5B       | MT1E        | LAX1        | SLC9A1      | PTK2        | C15orf57              | ERGIC2             | TERF2                                | CLEC12A         | APC                            | TAL1        |             |             |

## Bioinformatics Analysis of the Potential Regulatory Effects of miR-21 on MS-Associated Drug in Multiple Sclerosis

Table S3. GO enrichment (Cellular component pathway) analyses of 44 common differentially expressed genes (DEGs) with p<0.05

| Cellular component pathway ID                      | p-value     | Genes   |
|--|-------------|---|
| Microtubule minus-end (GO:0036449)                 | 1.31E-04    | <i>NIN; CAMSAP2</i>                           |
| Nuclear periphery (GO:0034399)                     | 6.74E-04    | <i>ATF7; SMC1A; DCAF7</i>                     |
| Microtubule end (GO:1990752)                       | 0.001062505 | <i>NIN; CAMSAP2</i>                           |
| Mitotic spindle pole (GO:0097431)                  | 0.001374107 | <i>NIN; SMC1A</i>                             |
| Membrane raft (GO:0045121)                         | 0.002276993 | <i>PIKFYVE; S100A10; TGFBR2</i>               |
| Nucleolus (GO:0005730)                             | 0.00344751  | <i>ATXN3; NIN; NRIP1; WDFY3; BRWD1; KDM7A</i> |
| Caveola (GO:0005901)                               | 0.006755543 | <i>ATP2B4; TGFBR2</i>                         |
| Nuclear matrix (GO:0016363)                        | 0.007474434 | <i>SMC1A; DCAF7</i>                           |
| Nucleoplasm part (GO:0044451)                      | 0.012080201 | <i>PHF20; IMPAD1; ARNT; DCAF7</i>             |
| Gamma-secretase complex (GO:0070765)               | 0.013129125 | <i>TMED10</i>                                 |
| Meiotic cohesin complex (GO:0030893)               | 0.013129125 | <i>SMC1A</i>                                  |
| Mitotic spindle (GO:0072686)                       | 0.014709297 | <i>NIN; SMC1A</i>                             |
| COPI-coated vesicle (GO:0030137)                   | 0.017467967 | <i>TMED10</i>                                 |
| Spindle pole (GO:0000922)                          | 0.023180005 | <i>NIN; SMC1A</i>                             |
| Nuclear inclusion body (GO:0042405)                | 0.023941303 | <i>ATXN3</i>                                  |
| Trans-Golgi network transport vesicle (GO:0030140) | 0.032507623 | <i>TMED10</i>                                 |
| NuRD complex (GO:0016581)                          | 0.034637697 | <i>GATAD2B</i>                                |
| pericentriolar material (GO:0000242)               | 0.034637697 | <i>NIN</i>                                    |
| CHD-type complex (GO:0090545)                      | 0.034637697 | <i>GATAD2B</i>                                |
| Nuclear body (GO:0016604)                          | 0.046308169 | <i>IMPAD1; ARNT; WDFY3; DCAF7</i>             |
| Histone acetyltransferase complex (GO:0000123)     | 0.047322234 | <i>PHF20</i>                                  |

Table S4. Biological process enrichment analyses of 44 common differentially expressed genes (DEGs) with p<0.05

| Biological process pathway ID   | p-value     | Genes                              |
|---|-------------|------------------------------------|
| Protein K63-linked deubiquitination (GO:0070536)  | 3.13E-05    | <i>ATXN3; TNFAIP3; BRCC3</i>       |
| Negative regulation of protein depolymerization (GO:1901880)  | 8.76E-04    | <i>LIM1; CAMSAP2</i>               |
| Protein K48-linked deubiquitination (GO:0071108)  | 0.001162071 | <i>ATXN3; TNFAIP3</i>              |
| Cellular response to interleukin-6 (GO:0071354)   | 0.001162071 | <i>ST3GAL6; IL6R</i>               |
| Regulation of interleukin-6 production (GO:0032675)   | 0.003851281 | <i>TNFAIP3; IL6R</i>               |
| Regulation of smooth muscle cell proliferation (GO:0048660)   | 0.004219716 | <i>TNFAIP3; IL6R</i>               |
| Negative regulation of supramolecular fiber organization (GO:1902904)                                     | 0.006294875 | <i>LIM1; CAMSAP2</i>               |
| Hemopoiesis (GO:0030097)  | 0.01215973  | <i>RTKN2; TGFBR2</i>               |
| Monoubiquitinated protein deubiquitination (GO:0035520)   | 0.013129125 | <i>ATXN3</i>                       |
| Regulation of epithelial to mesenchymal transition involved in endocardial cushion formation (GO:1905005) | 0.013129125 | <i>TGFBR2</i>                      |
| COPI-coated vesicle budding (GO:0035964)  | 0.013129125 | <i>TMED10</i>                      |
| Membrane raft assembly (GO:0001765)   | 0.013129125 | <i>S100A10</i>                     |
| Positive regulation of hormone metabolic process (GO:0032352)   | 0.013129125 | <i>ARNT</i>                        |
| COPI coating of Golgi vesicle (GO:0048205)  | 0.013129125 | <i>TMED10</i>                      |
| Regulation of T cell tolerance induction (GO:0002664)   | 0.013129125 | <i>TGFBR2</i>                      |
| Negative regulation of bone resorption (GO:0045779)   | 0.013129125 | <i>TNFAIP3</i>                     |
| Aggrephagy (GO:0035973)   | 0.013129125 | <i>WDFY3</i>                       |
| Response to DNA damage checkpoint signaling (GO:0072423)  | 0.013129125 | <i>SMC1A</i>                       |
| Protein deubiquitination involved in ubiquitin-dependent protein catabolic process (GO:0071947)           | 0.013129125 | <i>TNFAIP3</i>                     |
| Golgi transport vesicle coating (GO:0048200)  | 0.013129125 | <i>TMED10</i>                      |
| Regulation of cardiac muscle hypertrophy in response to stress (GO:1903242)                               | 0.013129125 | <i>ATP2B4</i>                      |
| Regulation of intracellular signal transduction (GO:1902531)  | 0.013642088 | <i>PHF20; FAM13A; TAGAP; AKAP7</i> |
| Negative regulation of nitric oxide biosynthetic process (GO:0045019)                                     | 0.015300881 | <i>ATP2B4</i>                      |
| Regulation of hormone biosynthetic process (GO:0046885)   | 0.015300881 | <i>ARNT</i>                        |
| Negative regulation of nitric oxide metabolic process (GO:1904406)  | 0.015300881 | <i>ATP2B4</i>                      |
| Response to misfolded protein (GO:0051788)  | 0.015300881 | <i>ATXN3</i>                       |
| Regulation of DNA endoreduplication (GO:0032875)  | 0.015300881 | <i>SMC1A</i>                       |
| Regulation of toll-like receptor 3 signaling pathway (GO:0034139)   | 0.015300881 | <i>TNFAIP3</i>                     |
| Positive regulation of CD4-positive, alpha-beta T cell activation (GO:2000516)                            | 0.015300881 | <i>TGFBR2</i>                      |

Table S4. contd.

| Biological process pathway ID  | p-value     | Genes                        |
|--|-------------|------------------------------|
| Regulation of transcription from RNA polymerase II promoter in response to oxidative stress (GO:0043619) | 0.017467967 | <i>ARNT</i>                  |
| Microtubule nucleation by microtubule organizing center (GO:0051418)                                     | 0.017467967 | <i>NIN</i>                   |
| Regulation of amyloid precursor protein catabolic process (GO:1902991)                                   | 0.017467967 | <i>TMED10</i>                |
| Calcium ion import across plasma membrane (GO:0098703)   | 0.017467967 | <i>ATP2B4</i>                |
| Response to epinephrine (GO:0071871)   | 0.017467967 | <i>ATP2B4</i>                |
| Regulation of toll-like receptor 2 signaling pathway (GO:0034135)  | 0.017467967 | <i>TNFAIP3</i>               |
| Histone H3-K36 demethylation (GO:0070544)  | 0.017467967 | <i>KDM7A</i>                 |
| Negative regulation of toll-like receptor 4 signaling pathway (GO:0034144)                               | 0.017467967 | <i>TNFAIP3</i>               |
| Positive regulation of alpha-beta T cell differentiation (GO:0046638)                                    | 0.017467967 | <i>TGFBF2</i>                |
| Negative regulation of monooxygenase activity (GO:0032769)   | 0.017467967 | <i>ATP2B4</i>                |
| Cellular response to epinephrine stimulus (GO:0071872)   | 0.017467967 | <i>ATP2B4</i>                |
| Negative regulation of bone remodeling (GO:0046851)  | 0.017467967 | <i>TNFAIP3</i>               |
| Calcium ion import into cytosol (GO:1902656)   | 0.017467967 | <i>ATP2B4</i>                |
| Regulation of ERAD pathway (GO:1904292)  | 0.017467967 | <i>ATXN3</i>                 |
| Proteolysis involved in cellular protein catabolic process (GO:0051603)                                  | 0.017827712 | <i>ATXN3; TNFAIP3</i>        |
| Protein deubiquitination (GO:0016579)  | 0.018853327 | <i>ATXN3; TNFAIP3; BRCC3</i> |
| B cell homeostasis (GO:0001782)  | 0.019630393 | <i>TNFAIP3</i>               |
| Atrioventricular valve development (GO:0003171)  | 0.019630393 | <i>TGFBF2</i>                |
| Microtubule anchoring at centrosome (GO:0034454)   | 0.019630393 | <i>NIN</i>                   |
| Golgi vesicle budding (GO:0048194)   | 0.019630393 | <i>TMED10</i>                |
| Protein modification by small protein removal (GO:0070646)   | 0.01963191  | <i>ATXN3; TNFAIP3; BRCC3</i> |
| Membrane raft organization (GO:0031579)  | 0.021788169 | <i>S100A10</i>               |
| Protein K11-linked deubiquitination (GO:0035871)   | 0.021788169 | <i>TNFAIP3</i>               |
| Myeloid dendritic cell differentiation (GO:0043011)  | 0.021788169 | <i>TGFBF2</i>                |
| Microtubule anchoring at microtubule organizing center (GO:0072393)                                      | 0.023941303 | <i>NIN</i>                   |
| Embryonic hemopoiesis (GO:0035162)   | 0.023941303 | <i>TGFBF2</i>                |
| Positive regulation of mesenchymal cell proliferation (GO:0002053)                                       | 0.023941303 | <i>TGFBF2</i>                |
| Negative regulation of cardiac muscle hypertrophy (GO:0010614)   | 0.023941303 | <i>ATP2B4</i>                |
| Regulation of actin filament depolymerization (GO:0030834)   | 0.023941303 | <i>LIMA1</i>                 |
| Response to sterol (GO:0036314)  | 0.023941303 | <i>TGFBF2</i>                |
| DNA repair (GO:0006281)  | 0.025350515 | <i>ATXN3; BRCC3; SMC1A</i>   |
| Regulation of mesenchymal cell proliferation (GO:0010464)  | 0.026089806 | <i>TGFBF2</i>                |
| Signal transduction involved in G2 DNA damage checkpoint (GO:0072425)                                    | 0.026089806 | <i>BRCC3</i>                 |
| Histone H3-K9 demethylation (GO:0033169)   | 0.026089806 | <i>KDM7A</i>                 |
| Vesicle budding from membrane (GO:0006900)   | 0.026089806 | <i>S100A10</i>               |
| Response to interleukin-6 (GO:0070741)   | 0.026089806 | <i>ST3GAL6</i>               |
| Positive regulation of vascular endothelial growth factor receptor signaling pathway (GO:0030949)        | 0.026089806 | <i>ARNT</i>                  |
| Negative regulation of reactive oxygen species biosynthetic process (GO:1903427)                         | 0.028233687 | <i>ATP2B4</i>                |
| Pathway-restricted SMAD protein phosphorylation (GO:0060389)   | 0.028233687 | <i>TGFBF2</i>                |
| Signal transduction involved in DNA damage checkpoint (GO:0072422)                                       | 0.028233687 | <i>BRCC3</i>                 |
| Positive regulation of ERAD pathway (GO:1904294)   | 0.028233687 | <i>ATXN3</i>                 |
| Regulation of cAMP-dependent protein kinase activity (GO:2000479)  | 0.028233687 | <i>ATP2B4</i>                |
| Positive regulation of alpha-beta T cell proliferation (GO:0046641)                                      | 0.028233687 | <i>TGFBF2</i>                |
| Branching involved in blood vessel morphogenesis (GO:0001569)  | 0.030372956 | <i>TGFBF2</i>                |
| Interleukin-6-mediated signaling pathway (GO:0070102)  | 0.030372956 | <i>IL6R</i>                  |
| Histone H4-K16 acetylation (GO:0043984)  | 0.030372956 | <i>PHF20</i>                 |
| Regulation of Golgi organization (GO:1903358)  | 0.030372956 | <i>CAMSAP2</i>               |
| Cardiac left ventricle morphogenesis (GO:0003214)  | 0.030372956 | <i>TGFBF2</i>                |
| Myeloid dendritic cell activation (GO:0001773)   | 0.030372956 | <i>TGFBF2</i>                |
| Regulation of defense response to virus (GO:0050688)   | 0.030372956 | <i>TNFAIP3</i>               |
| Regulation of synapse organization (GO:0050807)  | 0.030372956 | <i>PDLIM5</i>                |
| Regulation of calcineurin-NFAT signaling cascade (GO:0070884)  | 0.030372956 | <i>ATP2B4</i>                |
| Cytoskeleton organization (GO:0007010)   | 0.031356737 | <i>RTKN2; BRWD1</i>          |
| Atrioventricular valve morphogenesis (GO:0003181)  | 0.032507623 | <i>TGFBF2</i>                |
| Response to cholesterol (GO:0070723)   | 0.032507623 | <i>TGFBF2</i>                |
| Selective autophagy (GO:0061912)   | 0.032507623 | <i>WDFY3</i>                 |
| Histone H4-K8 acetylation (GO:0043982)   | 0.032507623 | <i>PHF20</i>                 |
| Phosphatidylethanolamine biosynthetic process (GO:0006646)   | 0.032507623 | <i>ETNK1</i>                 |
| Embryonic cranial skeleton morphogenesis (GO:0048701)  | 0.032507623 | <i>TGFBF2</i>                |
| Negative regulation of interleukin-2 production (GO:0032703)   | 0.032507623 | <i>TNFAIP3</i>               |
| Endocardial cushion morphogenesis (GO:0003203)   | 0.032507623 | <i>TGFBF2</i>                |
| Positive regulation of glycolytic process (GO:0045821)   | 0.032507623 | <i>ARNT</i>                  |
| Mitotic sister chromatid cohesion (GO:0007064)   | 0.032507623 | <i>SMC1A</i>                 |
| Response to X-ray (GO:0010165)   | 0.032507623 | <i>BRCC3</i>                 |
| Negative regulation of DNA-dependent DNA replication (GO:2000104)  | 0.032507623 | <i>SMC1A</i>                 |
| Histone H4-K5 acetylation (GO:0043981)   | 0.032507623 | <i>PHF20</i>                 |
| Positive regulation of coenzyme metabolic process (GO:0051197)   | 0.032507623 | <i>ARNT</i>                  |

Bioinformatics Analysis of the Potential Regulatory Effects of miR-21 on MS-Associated Drug in Multiple Sclerosis

Table S4. contd.

| Biological process pathway ID   | p-value     | Genes                        |
|---|-------------|------------------------------|
| Negative regulation of translational initiation (GO:0045947)                                    | 0.034637697 | <i>EIF4EBP2</i>              |
| Sialylation (GO:0097503)  | 0.034637697 | <i>ST3GAL6</i>               |
| Regulation of toll-like receptor 4 signaling pathway (GO:0034143)                               | 0.034637697 | <i>TNFAIP3</i>               |
| Ruffle organization (GO:0031529)  | 0.034637697 | <i>LIMA1</i>                 |
| mRNA transcription from RNA polymerase II promoter (GO:0042789)                                 | 0.034637697 | <i>ARNT</i>                  |
| Regulation of cell cycle phase transition (GO:1901987)  | 0.034637697 | <i>ATP2B4</i>                |
| Positive regulation of response to endoplasmic reticulum stress (GO:1905898)                    | 0.034637697 | <i>ATXN3</i>                 |
| Positive regulation of focal adhesion assembly (GO:0051894)                                     | 0.036763188 | <i>S100A10</i>               |
| Septin ring organization (GO:0031106)   | 0.036763188 | <i>RTKN2</i>                 |
| Negative regulation of B cell activation (GO:0050869)   | 0.036763188 | <i>TNFAIP3</i>               |
| Regulation of small GTPase mediated signal transduction (GO:0051056)                            | 0.038004345 | <i>FAM13A; TAGAP</i>         |
| Negative regulation of microtubule depolymerization (GO:0007026)                                | 0.038884106 | <i>CAMSAP2</i>               |
| Membrane lipid metabolic process (GO:0006643)   | 0.038884106 | <i>ST3GAL6</i>               |
| Regulation of microtubule polymerization or depolymerization (GO:0031110)                       | 0.038884106 | <i>CAMSAP2</i>               |
| Positive regulation of carbohydrate metabolic process (GO:0045913)                              | 0.038884106 | <i>ARNT</i>                  |
| Regulation of amyloid-beta formation (GO:1902003)   | 0.038884106 | <i>TMED10</i>                |
| Regulation of chemokine production (GO:0032642)   | 0.038884106 | <i>IL6R</i>                  |
| Acute-phase response (GO:0006953)   | 0.038884106 | <i>IL6R</i>                  |
| Negative regulation of calcium-mediated signaling (GO:0050849)                                  | 0.038884106 | <i>ATP2B4</i>                |
| Cell-cell adhesion via plasma-membrane adhesion molecules (GO:0098742)                          | 0.038994651 | <i>CLDN8; TGFB2</i>          |
| Regulation of mitotic spindle assembly (GO:1901673)   | 0.04100046  | <i>SMC1A</i>                 |
| Cellular response to interleukin-7 (GO:0098761)   | 0.04100046  | <i>BRWD1</i>                 |
| Regulation of protein kinase A signaling (GO:0010738)   | 0.04100046  | <i>AKAP7</i>                 |
| Purine ribonucleoside bisphosphate metabolic process (GO:0034035)                               | 0.04100046  | <i>IMPAD1</i>                |
| Histone deubiquitination (GO:0016578)   | 0.04100046  | <i>BRCC3</i>                 |
| Negative regulation of lymphocyte activation (GO:0051250)                                       | 0.04100046  | <i>TNFAIP3</i>               |
| Positive regulation of adherens junction organization (GO:1903393)                              | 0.04100046  | <i>S100A10</i>               |
| Protein heterotetramerization (GO:0051290)  | 0.04100046  | <i>S100A10</i>               |
| Calcium ion transport into cytosol (GO:0060402)   | 0.04100046  | <i>ATP2B4</i>                |
| Interleukin-7-mediated signaling pathway (GO:0038111)   | 0.04100046  | <i>BRWD1</i>                 |
| Negative regulation of innate immune response (GO:0045824)                                      | 0.043112259 | <i>TNFAIP3</i>               |
| Regulation of vacuole organization (GO:0044088)   | 0.043112259 | <i>PIKfyve</i>               |
| Cellular response to estradiol stimulus (GO:0071392)  | 0.043112259 | <i>NRIP1</i>                 |
| Phosphatidylethanolamine metabolic process (GO:0046337)   | 0.043112259 | <i>ETNK1</i>                 |
| Calcium-independent cell-cell adhesion via plasma membrane cell-adhesion molecules (GO:0016338) | 0.043112259 | <i>CLDN8</i>                 |
| mRNA transcription (GO:0009299)   | 0.045219514 | <i>ARNT</i>                  |
| Dendritic cell differentiation (GO:0097028)   | 0.045219514 | <i>TGFB2</i>                 |
| Regulation of interleukin-2 production (GO:0032663)   | 0.045219514 | <i>TNFAIP3</i>               |
| Ventricular septum morphogenesis (GO:0060412)   | 0.045219514 | <i>TGFB2</i>                 |
| Cellular response to misfolded protein (GO:0071218)   | 0.045219514 | <i>ATXN3</i>                 |
| Histone lysine demethylation (GO:0070076)   | 0.045219514 | <i>KDM7A</i>                 |
| Embryonic skeletal system morphogenesis (GO:0048704)  | 0.045219514 | <i>TGFB2</i>                 |
| Cellular macromolecule biosynthetic process (GO:0034645)  | 0.04668864  | <i>EIF4EBP2; ARNT; RBMS1</i> |
| Regulation of microtubule depolymerization (GO:0031114)   | 0.047322234 | <i>CAMSAP2</i>               |
| Regulation of vascular endothelial growth factor receptor signaling pathway (GO:0030947)        | 0.047322234 | <i>ARNT</i>                  |
| Regulation of bone resorption (GO:0045124)  | 0.047322234 | <i>TNFAIP3</i>               |
| Positive regulation of erythrocyte differentiation (GO:0045648)                                 | 0.047322234 | <i>ARNT</i>                  |
| Outflow tract septum morphogenesis (GO:0003148)   | 0.047322234 | <i>TGFB2</i>                 |
| Negative regulation of intracellular signal transduction (GO:1902532)                           | 0.048879819 | <i>ATP2B4; TNFAIP3</i>       |
| Positive regulation of ATP metabolic process (GO:1903580)                                       | 0.049420428 | <i>ARNT</i>                  |
| Cellular response to catecholamine stimulus (GO:0071870)  | 0.049420428 | <i>ATP2B4</i>                |
| Positive regulation of cell junction assembly (GO:1901890)                                      | 0.049420428 | <i>S100A10</i>               |
| Membrane assembly (GO:0071709)  | 0.049420428 | <i>S100A10</i>               |
| Regulation of dendritic spine morphogenesis (GO:0061001)  | 0.049420428 | <i>PDLIM5</i>                |
| TOR signaling (GO:0031929)  | 0.049420428 | <i>EIF4EBP2</i>              |



Table S5. Molecular functions enrichment analyses of 44 common differentially expressed genes (DEGs) with p&lt;0.05

| Molecular function pathway ID  | p-value     | Genes                        |
|--|-------------|------------------------------|
| Lys63-specific deubiquitinase activity (GO:0061578)  | 1.62E-06    | <i>ATXN3; TNFAIP3; BRCC3</i> |
| Ubiquitin-like protein-specific protease activity (GO:0019783)                                     | 5.77E-04    | <i>ATXN3; TNFAIP3; BRCC3</i> |
| Thiol-dependent ubiquitin-specific protease activity (GO:0004843)                                  | 6.24E-04    | <i>ATXN3; TNFAIP3; BRCC3</i> |
| Thiol-dependent ubiquitinyl hydrolase activity (GO:0036459)  | 0.001088282 | <i>ATXN3; TNFAIP3; BRCC3</i> |
| Polyubiquitin modification-dependent protein binding (GO:0031593)                                  | 0.004033525 | <i>TNFAIP3; BRCC3</i>        |
| Protein phosphatase 2B binding (GO:0030346)  | 0.013129125 | <i>ATP2B4</i>                |
| Transforming growth factor beta-activated receptor activity (GO:0005024)                           | 0.013129125 | <i>TGFBR2</i>                |
| 1-phosphatidylinositol-4-phosphate 5-kinase activity (GO:0016308)                                  | 0.013129125 | <i>PIKFYVE</i>               |
| Interleukin-6 receptor binding (GO:0005138)  | 0.015300881 | <i>IL6R</i>                  |
| Adenylate kinase activity (GO:0004017)   | 0.015300881 | <i>AK2</i>                   |
| Beta-galactoside (CMP) alpha-2,3-sialyltransferase activity (GO:0003836)                           | 0.015300881 | <i>ST3GAL6</i>               |
| Type I transforming growth factor beta receptor binding (GO:0034713)                               | 0.017467967 | <i>TGFBR2</i>                |
| Aryl hydrocarbon receptor binding (GO:0017162)   | 0.017467967 | <i>ARNT</i>                  |
| Glucocorticoid receptor binding (GO:0035259)   | 0.019630393 | <i>NRIP1</i>                 |
| Histone demethylase activity (H3-K36 specific) (GO:0051864)  | 0.019630393 | <i>KDM7A</i>                 |
| Phosphatidylinositol binding (GO:0035091)  | 0.020429484 | <i>SNX13; WDFY3</i>          |
| Lys48-specific deubiquitinase activity (GO:1990380)  | 0.021788169 | <i>ATXN3</i>                 |
| Microtubule minus-end binding (GO:0051011)   | 0.021788169 | <i>CAMSAP2</i>               |
| Eukaryotic initiation factor 4E binding (GO:0008190)   | 0.021788169 | <i>EIF4EBP2</i>              |
| Histone acetyltransferase activity (H4-K16 specific) (GO:0046972)                                  | 0.021788169 | <i>PHF20</i>                 |
| Histone acetyltransferase activity (H4-K5 specific) (GO:0043995)                                   | 0.021788169 | <i>PHF20</i>                 |
| Histone acetyltransferase activity (H4-K8 specific) (GO:0043996)                                   | 0.021788169 | <i>PHF20</i>                 |
| Nitric-oxide synthase binding (GO:0050998)   | 0.023941303 | <i>ATP2B4</i>                |
| Histone demethylase activity (H3-K9 specific) (GO:0032454)   | 0.028233687 | <i>KDM7A</i>                 |
| Phosphatidylinositol phosphate 5-phosphatase activity (GO:0034595)                                 | 0.028233687 | <i>PIKFYVE</i>               |
| Transmembrane receptor protein serine/threonine kinase activity (GO:0004675)                       | 0.030372956 | <i>TGFBR2</i>                |
| Calcium-transporting ATPase activity (GO:0005388)  | 0.030372956 | <i>ATP2B4</i>                |
| 1-phosphatidylinositol binding (GO:0005545)  | 0.030372956 | <i>WDFY3</i>                 |
| Phosphatidylinositol-3,5-bisphosphate phosphatase activity (GO:0106018)                            | 0.032507623 | <i>PIKFYVE</i>               |
| Phosphatidylinositol phosphate kinase activity (GO:0016307)  | 0.032507623 | <i>PIKFYVE</i>               |
| Nucleotidase activity (GO:0008252)   | 0.034637697 | <i>IMPAD1</i>                |
| H4 histone acetyltransferase activity (GO:0010485)   | 0.036763188 | <i>PHF20</i>                 |
| GTP-Rho binding (GO:0017049)   | 0.036763188 | <i>RTKN2</i>                 |
| Protein kinase A regulatory subunit binding (GO:0034237)   | 0.038884106 | <i>AKAP7</i>                 |
| Transforming growth factor beta binding (GO:0050431)   | 0.04100046  | <i>TGFBR2</i>                |
| Cadherin binding involved in cell-cell adhesion (GO:0098641)                                       | 0.04100046  | <i>PDLIM5</i>                |
| Mitogen-activated protein kinase binding (GO:0051019)  | 0.043112259 | <i>ATF7</i>                  |
| K63-linked polyubiquitin modification-dependent protein binding (GO:0070530)                       | 0.043112259 | <i>TNFAIP3</i>               |
| Sialyltransferase activity (GO:0008373)  | 0.045219514 | <i>ST3GAL6</i>               |
| Protein binding involved in cell-cell adhesion (GO:0098632)  | 0.045219514 | <i>PDLIM5</i>                |
| ATPase activity, coupled to transmembrane movement of ions, phosphorylative mechanism (GO:0015662) | 0.047322234 | <i>ATP2B4</i>                |
| Actinin binding (GO:0042805)   | 0.047322234 | <i>PDLIM5</i>                |
| Nucleotide kinase activity (GO:0019201)  | 0.049420428 | <i>AK2</i>                   |